Frontiers in Heat and Mass Transfer (FHMT), 9, 40 (2017)
DOI: 10.5098/hmt.9.40

Global Digital Central
ISSN: 2151-8629

Frontiers in Heat and Mass Transfer

Available at www.ThermalFluidsCentral.org

ENTROPY GENERATION OF UNSTEADY RADIATIVE CASSON FLUID FLOW THROUGH POROUS MEDIUM OVER A PERMEABLE STRETCHING SURFACE WITH INCLINED MAGNETIC FIELD

Shalini Jain* Amit Parmar

Department of Mathematics and Statistics, Manipal University, Rajasthan, India

ABSTRACT

Present paper aims to investigate entropy generation of unsteady radiative Casson fluid flow through porous medium over a permeable stretching surface with inclined magnetic field. Time-dependent partial differential equations are transformed into non-linear ordinary differential equations using similarity transformations. These transformed equations are solved numerically by Runge–Kutta fourth-order with shooting technique. The effects of pertinent parameter such as magnetic field parameter, Casson fluid parameter, inclined angle of magnetic field parameter, Radiation parameter and Reynolds number on the velocity, temperature and entropy profiles are presented graphically. Local Nusselt and local Sherwood number are also obtained and presented in tabulated form.

Keyword *Unsteady boundary layer, Casson fluid, starching surface, inclined magnetic field, entropy generation.*

1. INTRODUCTION

The study of heat transfer and entropy generation over stretching sheet for under different physical conditions has attracted the attention of researcher's due to their various applications in engineering/industrial disciplines. These applications include extrusion processes, wire and fiber coating, polymer processing, food-stuff processing, and design of heat exchangers and chemical processing equipment, in glass fiber, metal extrusion, materials handling conveyors, production of plastic and rubber, cooling, temperature exchangers, and turbo machinery. Due to the presence of temperature gradient every thermal process has some kind of irreversibility and entropy generation is the measure of irreversibility of the system. It causes efficiency loss and reduction of quality. Chauhan et al. (2011a, 2011b, 2011c) investigated second law analyzed during compressible fluid flow in a partially filled channel, stretching sheet and annular pipe with a porous medium and MHD effect. Jain et al. (2017a) examined entropy Generation for MHD Radiation effect on viscous fluid in a partially filled channel. Entropy generation minimization has been investigated by several researchers several researchers (Bejan (1996), Jangili et al. (2016), Qing et al. (2016) and Bhatti et al. (2016)) for both Newtonian and non-Newtonian fluid over different geometries

Jet al. (2012, 2013, 2014) investigated the flow and heat transfer for geometries including stretching sheet, stretching cylinder, porous oscillating plate under different set of physical and thermal boundary conditions. Effects of radiation and porosity on non-Newtonian fluid flow have many important applications in the field of science and engineering including effects to controlling heat transfer in polymer processing industry where the quality of the final product depends, to some extent, on heat controlling factors. High-temperature plasma, nuclear reactors, liquid metal fluids and power generation systems are some of the important applications of radiative heat transfer of conductive gray fluids flow over a vertical wall. Radiative Casson flow, heat and mass transfer over a circular cylinder in presence of porous medium investigated by Mabood et al. (2015). Jain and Choudhary (2017) examined Soret and Dufour effects on MHD fluid flow due to moving permeable cylinder with radiation. Degan, et al. (2007) investigated non-Newtonian fluids flow over a vertical surface embedded in an anisotropic porous medium. Jain et al. (2006 and 2015) studied viscous and MHD fluid flow over a stretching sheet and exponentially shrinking sheet with slip condition. Jain and Bohra (2017) investigated flow and heat transfer inclined non linear stretching sheet under convective boundary conditions. Jain et al. (2018a, 2018b) investigated fluid flow and heat transfer with radiation for squeezing nanofluid in a rotating channel and Williamson nanofluid over a stretching cylinder. Reddy (2015) studied unsteady radiative Casson fluid with convective boundary-layer condition and variable thermal conductivity.

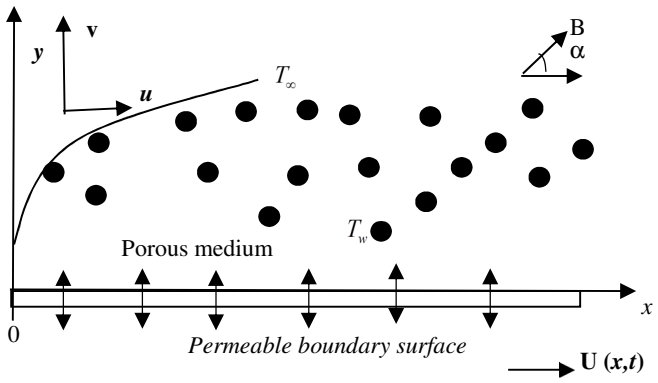

Fig. 1 Geometric scheme of the problem.

The current study aimed to examine entropy generation of unsteady radiative Casson fluid flow through porous medium over a permeable stretching surface with inclined magnetic field. The flow and heat transfer characteristics are analyzed and displayed graphically and in

* Corresponding author. Email: shalini.jain@jaipur.manipal.edu

Global Digital Central
ISSN: 2151-8629

tabulated form. Oueslati and Beya (2017a, 2017b, 2017c) examined the effects of magnetic and thermosolutal natural convection with entropy generation. Kolsi (2016) analysed MHD mixed convection with entropy .

2. FORMULATION OF PROBLEM

Consider two-dimensional, unsteady radiative Casson fluid flow through porous medium over a permeable stretching surface with inclined magnetic field. Flow is induced by stretching of a surface along x axis moving with non-uniform velocity $U(x,t) = cx/(1-\gamma t)$ where $c > 0,\ \gamma \geq 0$. The velocity component along x and y axis are u and v. Temperature T depends on x and time t. A uniform inclined magnetic field is applied at an angle α to the fluid flow. On the flow field, no applied voltage or polarization voltage is imposed, therefore electric field $\vec{E} = 0$ therefore Joule heating, viscous dissipation and Hall current effects are neglected. The rheological equation of state, for an isotropic and incompressible flow of a Casson fluid is as follows:

$$\tau_{ij} = \begin{cases} 2(\mu_B + p_y/\sqrt{2\pi})e_{ij}, & \pi > \pi_c \\ 2(\mu_B + p_y/\sqrt{2\pi_c})e_{ij}, & \pi < \pi_c \end{cases}$$

Where τ_{ij} is the (i, j)-th component of the stress tensor, π is the product of the component of the deformation rate with itself, π_c is a critical value of this product based on the non-Newtonian model, μ_B is plastic dynamic viscosity of the non-Newtonian Casson fluid, and p_y is the yield stress of the fluid. When stress is greater than the yield stress fluid starts to move under the force going assumption, the governing equation of such type of flow are

The continuity, momentum and energy equations governing the fluid flow are given by

$$\frac{\partial u}{\partial x} + \frac{\partial v}{\partial y} = 0 \tag{1}$$

$$\frac{\partial u}{\partial t} + u\frac{\partial u}{\partial x} + v\frac{\partial u}{\partial y} = \nu\left(1 + \frac{1}{\beta}\right)\frac{\partial^2 u}{\partial y^2} - \frac{\sigma B^2 \sin^2\alpha}{\rho}u - \nu\frac{u}{k_p} \tag{2}$$

$$\frac{\partial T}{\partial t} + u\frac{\partial T}{\partial x} + v\frac{\partial T}{\partial y} = \frac{k}{\rho C_p}\frac{\partial^2 T}{\partial y^2} + \frac{\sigma B^2 \sin^2\alpha}{\rho C_p}u^2 - \frac{1}{\rho C_p}\frac{\partial q_r}{\partial y} \tag{3}$$

The boundary conditions are given as

$$\begin{aligned} &at\ y = 0; \quad u = U(x,t), \quad v = -v_w, \quad T = T_W(x,t) \\ &y \to \infty; \quad u \to 0, \quad T \to T_\infty \end{aligned} \tag{4}$$

Where u and v are the components of velocity, respectively, in the *x* and *y* direction, ν is the kinematic viscosity of the fluid, k is the thermal conductivity, k_p permeability of the medium and ρ is the viscosity, C_p is the specific heat and B is the magnetic field. On expanding T^4, in a Taylor series about T_∞, on neglecting higher order term, we get

$$T^4 \approx {T_\infty}^4 + 4{T_\infty}^3 T - 4{T_\infty}^3 T_\infty$$

$$\frac{\partial q_r}{\partial y} = \frac{\partial}{\partial y}\left(\frac{-4\sigma}{3k^*}\frac{\partial T^4}{\partial y}\right) = \frac{\partial}{\partial y}\left(\frac{-4\sigma}{3k^*}\frac{\partial({T_\infty}^4 + 4{T_\infty}^3 T - 4{T_\infty}^3 T_\infty)}{\partial y}\right)$$

$$= \frac{-16\sigma {T_\infty}^3}{3k^*}\frac{\partial^2 T}{\partial y^2}$$

and now

$$\frac{\partial u}{\partial x} + \frac{\partial v}{\partial y} = 0$$

$$\frac{\partial u}{\partial t} + u\frac{\partial u}{\partial x} + v\frac{\partial u}{\partial y} = \nu\left(1 + \frac{1}{\beta}\right)\frac{\partial^2 u}{\partial y^2} - \frac{\sigma B^2 \sin^2\alpha}{\rho}u - \nu\frac{u}{k_p}$$

$$\frac{\partial T}{\partial t} + u\frac{\partial T}{\partial x} + v\frac{\partial T}{\partial y} = \frac{k}{\rho C_p}\frac{\partial^2 T}{\partial y^2} + \frac{\sigma B^2 sin^2\alpha}{\rho C_p}u^2 - \frac{1}{\rho C_p}\frac{(-16\sigma {T_\infty}^3)}{3k^*}\frac{\partial^2 T}{\partial y^2}$$

T is the temperature, $T_W(x,t) = T_\infty + \frac{cx^2 T_0(1-\gamma t)^{-3/2}}{2\nu}$, where T_0, is a reference temperature T_∞, is a constant free stream temperature. $\beta = \mu_B\sqrt{2\pi_c}/p_y$ is the Casson fluid parameter. The expression for $U(x,t)$ and $T_W(x,t)$ are valid for the time $t < \gamma^{-1}$

3. GOVERNING EQUATIONS AND BOUNDARY CONDITIONS

Introduce the following relations for u, v as

$$u = \frac{\partial \psi}{\partial y}, \quad v = -\frac{\partial \psi}{\partial x}, \tag{5}$$

Where Ψ(x, y) is the stream function. The governing equations are converted into non- dimensional form, introduce the following similarity transformation:

$$\psi = \left(\frac{\nu c}{1-\gamma t}\right)^{\frac{1}{2}} x f(\eta), \quad \eta = \left(\frac{c}{\nu(1-\gamma t)}\right)^{\frac{1}{2}} y, \quad \theta = \frac{T - T_\infty}{T_W - T_\infty}. \tag{6}$$

On using equation (5) and (6), we obtain velocity components in non-dimensional form as given below:

$$u = \frac{c}{(1-\gamma t)} x f'(\eta), \qquad v = -\left(\frac{\nu c}{1-\gamma t}\right)^{\frac{1}{2}} f(\eta). \tag{7}$$

Equation (2) and (3) thus reduces in the equation (8) and (9)

$$\left(1 + \frac{1}{\beta}\right)f''' + ff'' - f'^2 - A\left(f' + \frac{\eta}{2}f''\right) - M^2 f' sin^2\alpha - \frac{f'}{Da\,\mathrm{Re}} = 0 \tag{8}$$

$$\frac{1}{\mathrm{Pr}}(\theta'' + \frac{4R}{3}\theta'') + f\theta' - 2f'\theta + M^2 sin^2\alpha\, Ecf'^2 - A\left(\frac{3}{2}\theta + \frac{\eta}{2}\theta'\right) = 0 \tag{9}$$

with the boundary conditions (4) becomes

$$\begin{aligned} &\eta \to 0 : f'(\eta) = 1, \ f(\eta) = S, \ \theta(\eta) = 1, \\ &\eta \to \infty : f'(\eta) \to 0, \ \theta(\eta) \to 0 \end{aligned} \tag{10}$$

Where, $A = \frac{\gamma}{c}$ is the unsteadiness parameter, $M^2 = \frac{\sigma B^2(1-\gamma t)}{\rho c}$ is magnetic field parameter, $\mathrm{Pr} = \mu C_p/k$ is the Prandtl number, $R = \frac{4\sigma {T_\infty}^3}{kk^*}$ is the Radiation parameter, k is the thermal radiation parameter, $Ec = \frac{U^2}{C_p(T_W - T_\infty)}$ is Eckert number, $Da = \frac{K_p}{x^2}$ is Darcy number, $\mathrm{Re} = \frac{xU}{\nu}$ is Reynolds number, $S = v_w\left(\frac{1-\gamma t}{\nu c}\right)^{\frac{1}{2}}$: suction/injection parameter.

Global Digital Central
ISSN: 2151-8629

4. NUMERICAL SOLUTION

The equation (8), (9) and (10) are solved by Runge-Kutta fourth-order together with shooting method. After suitable transformations, the boundary value problem is transform to the following system of initial value problems

$$f' = z, \qquad z' = p,$$

$$p' = \frac{1}{\left(1+\frac{1}{\beta}\right)}\left[A\left(z+\frac{\eta}{2}p\right)+z^2+zM^2\sin^2(\alpha)-fp\right]$$

$$\theta' = q,$$

$$q' = \left(\frac{\Pr}{1+\frac{4}{3}R}\right)\left(2f'\theta - fq + A\left(\frac{3}{2}\theta+\frac{\eta}{2}q\right)-Ec\,M^2p^2\right) \tag{11}$$

with the boundary conditions

$$f = S, \quad z = 1, \quad \theta = 1, \quad at \quad \eta = 0 \tag{12}$$
$$f' \to 0 \quad \theta \to 0 \quad at \quad \eta \to \infty$$

Characteristics of flow are the skin friction coefficient c_f and the Nusselt number Nu_x, respectively defined as (Mabood et al. 2015)

$$c_f = \left(1+\frac{1}{\beta}\right)\frac{\tau_w}{\rho U^2}, \qquad \text{and} \qquad Nu_x = \frac{xq_w}{k_\infty(T_w - T_\infty)}, \tag{13}$$

where the skin friction τ w and the heat flux q_w on the sheet are

$$\tau_w = \mu\left(\frac{\partial u}{\partial y}\right)_{y=0} \text{ and } \quad q_w = -k_\infty\left(1+\frac{4}{3}R\right)\frac{\partial T}{\partial y}_{y=0} \tag{14}$$

The dimensionless expressions for the skin friction coefficient and Nusselt number are the following.

$$c_f \,\mathrm{Re}_x^{\frac{1}{2}} = \left(1+\frac{1}{\beta}\right)f''(0), \qquad \text{and} \quad Nu\,\mathrm{Re}_x^{\frac{1}{2}} = -\left(1+\frac{4}{3}R\right)\theta'(0), \tag{15}$$

5. ENTROPY GENERATION ANALYSIS

The volumetric rate of local entropy generation of the Casson fluid over the stretching sheet (Qing et al. (2016))

$$S_{gen} = \frac{k}{T_\infty^2}\left(1+\frac{4}{3}R\right)\left(\frac{\partial T}{\partial y}\right)^2 + \frac{\mu}{T_\infty}\left(1+\frac{1}{\beta}\right)\left(\frac{\partial u}{\partial y}\right)^2 + \frac{\sigma B^2 sin^2\alpha}{T_\infty}u^2 \tag{16}$$

Here the first, second and third term on the right hand is present the local entropy generation due to heat transfer, local entropy generation due to Casson fluid effect and local entropy generation due to inclined magnetic dissipation effect.

We know that characteristic entropy generation rate is

$$(S_{gen})_o = \frac{k(\Delta T)^2}{T_\infty^2 x^2} \tag{17}$$

In order to get the non-dimensional form of entropy generation we used the similarity transformation parameters of equation (6). Hence dimensionless entropy generation equation is

$$N_S = \frac{S_{gen}}{(S_{gen})_o} \tag{18}$$

Equation (16), (17) and (18) are reduced to:

$$N_S = \mathrm{Re}\left(1+\frac{4}{3}R\right)\theta'^2 + \left(1+\frac{1}{\beta}\right)\frac{Br\,\mathrm{Re}\,f''^2}{\Omega} + \frac{Br\,M^2 sin^2\alpha\,\mathrm{Re}\,f'^2}{\Omega}. \tag{19}$$

Here $Br = \frac{\mu(U_w(x,t))^2}{K_\infty(\Delta T)}$; Brinkman number, $\Omega = \frac{\Delta T}{T_\infty}$; dimensionless temperature difference.

6. RESULTS AND DISCUSSION

Figures 2-21 describe the effect of pertinent parameters on velocity, temperature and entropy profiles. It is observed that the result obtained in present study are well in agreement with the results obtained by Reddy et al. (2015). Figs. (2-5) show effects of Casson fluid parameter β, unsteadiness parameter A, magnetic field parameter M, and inclined magnetic field angle α on velocity profile. It is observed that boundary layer thickness and velocity decreases as A, β, M and α increases. Because of the increase in Casson parameter β, the yield stress reduces as a result the momentum boundary layer thickness decreases. Figs. (6-7) depicts that velocity increases as Darcy number Da and Reynolds number Re increases. Figs. (8- 12) depicts that as Casson fluid parameter β, magnetic field parameter M, inclined magnetic field angle α, radiation parameter R and Eckert number Ec increases, temperature as well as thermal boundary layer thickness increases. Physically, increasing the values of Ec enhances the temperature within the fluid flow because heat generates in the fluid due to frictional heating. Figs. (13) - (14) show that as unsteadiness parameter A and Prandtl number Pr increase, temperature as well as thermal boundary layer thickness deceases. Prandtl number signifies the ratio of momentum diffusivity to thermal diffusivity. Fluids with lower Prandtl number will possess higher thermal conductivities, so that heat can diffuse from the sheet faster than for higher Pr fluids. Prandtl number increases the rate of cooling in conducting flows. Figs. (15) - (16) show that as suction/injection parameter increase, temperature and velocity profile as well as momentum boundary thickness and thermal boundary layer deceases. Actually, the effect of suction is to make the velocity and temperature distribution more uniform within the boundary layer. Imposition of fluid suction at the surface has a tendency to reduce both the hydrodynamic and the thermal thickness of the boundary layer where viscous effects dominate. This has the effect of reducing both the fluid velocity and the temperature. On the other hand, the thermal boundary layer thickness increases with injection which causes a decrease in the rate of heat transfer. Figs. (17) - (23) show that an increase in unsteady parameter, Magnetic field parameter, Reynolds number, Brinkman number, radiation parameter, and inclined angle of magnetic field parameter increases the entropy profile and whereas reverses effect has been observed on the increases of Casson fluid parameter. Entropy function strongly depends upon Reynolds number. With high Reynolds number, hectic motion occurs because as Re increases, the fluid moves more disturbingly and thus contribution of fluid friction and heat transfer on entropy result tends to increase in entropy generation. Table 1 shows the influence of various physically parameter on skin friction coefficient and Nusselt number. Rising the value of unsteady parameter and magnetic field parameter, reduces the skin friction coefficient and revers impact show of unsteady parameter on Nusselt number. Increasing Casson fluid parameter rising the skin friction coefficient and reduces the value of Nusselt number. Tables 2 give a comparison of the skin friction coefficient for various values of the unsteadiness parameter A for a Newtonian fluid with the previously published results.

Table 1 Numerical value of skin friction coefficient and Nusselt number

β =2, A=0.5, Re=1, Da=2, Br=1.5, $\alpha = \pi/6$, Pr=2.0, R=0.5, Ec=1.5, M=1, S=0.									
α	A	β	M	Ec	R	S	Re	$c_f \mathrm{Re}_x^{\frac{1}{2}}$	$Nu\,\mathrm{Re}_x^{\frac{1}{2}}$
	0							-1.8893	2.7806
	1							-2.1877	3.5585
	2							-2.4573	4.1802
		0.8						-2.4393	3.2445
		1						-2.3154	3.2319
		2						-2.0420	3.1955
			0					-1.9330	3.4115
			1					-2.0420	3.1955
			2					-2.1445	2.9938
				0				-	3.3906
				2				-	3.1305
				4				-	2.8703
					0			-	2.6567
					1			-	3.6141
					2			-	4.2657
						-0.5		-1.5574	2.2245
						0		-1.7823	2.6612
						0.5		-2.0420	3.1955
$\frac{\pi}{6}$								-1.9330	3.4115
$\frac{\pi}{4}$								-2.0420	3.1955
$\frac{\pi}{3}$								-2.2417	2.8039
							0.02	-6.5739	2.7316
							0.2	-2.7451	3.1056
							2	-1.9330	3.2092

Table 2 The values off "(0) various values of unsteadiness parameter A

$\beta \to \infty$ =2, Da $\to \infty$, $\alpha = \pi/2$, M=0. Re $\to \infty$					
A	*Oyelakin et al. (2016)*	*Sharidan et al (2006)*	*Chamka et al. (2010)*	*Layek, et al. (2013)*	*Present study*
0.8	1.261043	1.261042	1.261512	1.261479	1.2610466
1.2	1.377725	1.377722	1.378052	1.377850	1.3777331

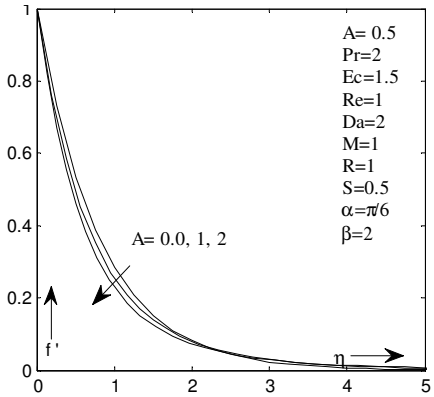

Fig. 2 Velocity profile for unsteadiness parameter A

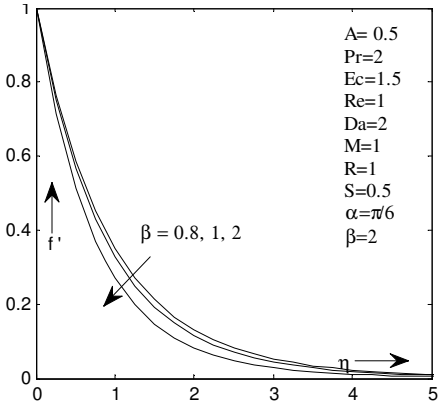

Fig. 3 Velocity profile for Casson parameter β

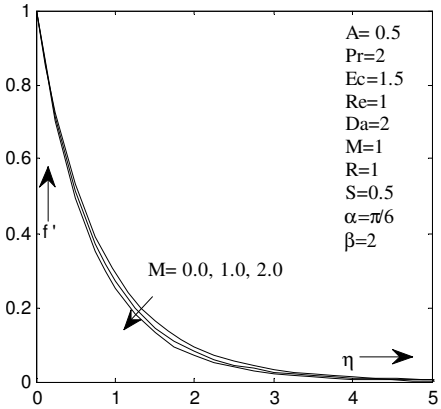

Fig. 4 Velocity profile for Magnetic field parameter M

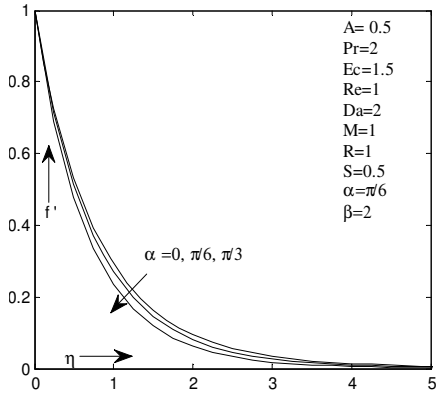

Fig. 5 Velocity profile for inclined angle α

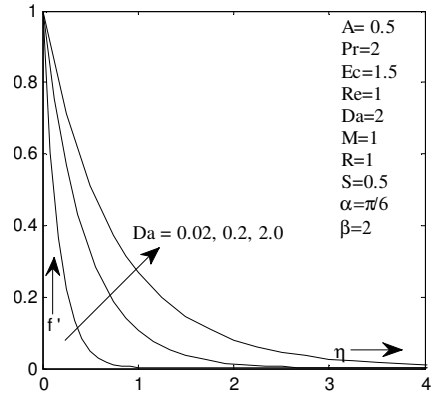

Fig. 6 Velocity profile for Darcy number

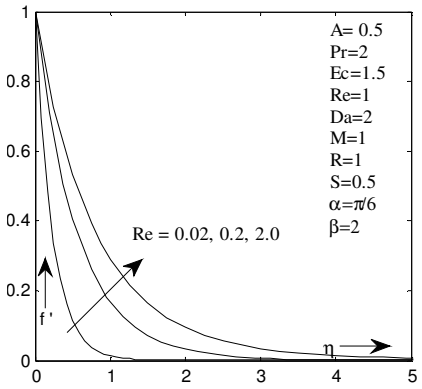

Fig. 7 Velocity profile for Re

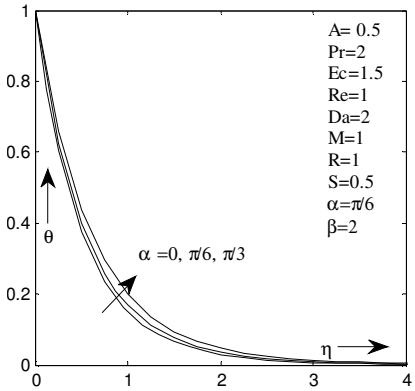

Fig. 11 Temperature profile for parameter α

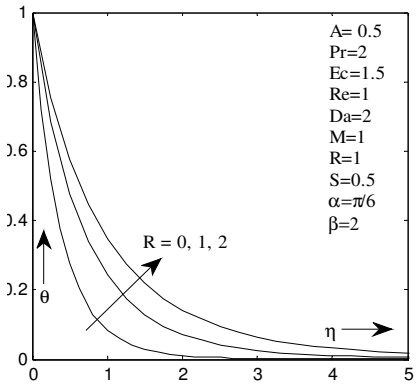

Fig. 8 Temperature profile for parameter R

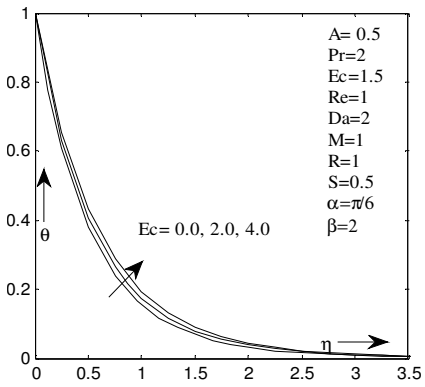

Fig. 12 Temperature profile for parameter Ec

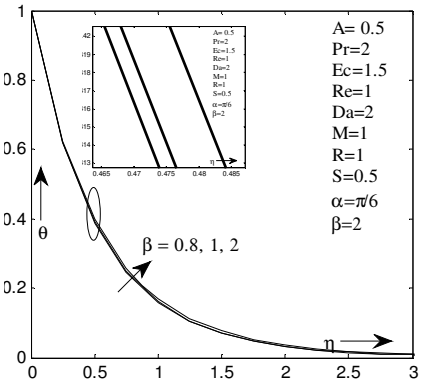

Fig. 9 Temperature profile for parameter β

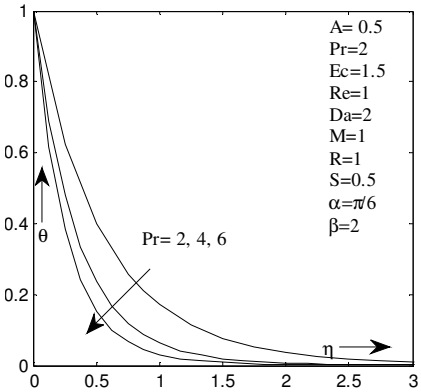

Fig. 13 Temperature profile for parameter Pr

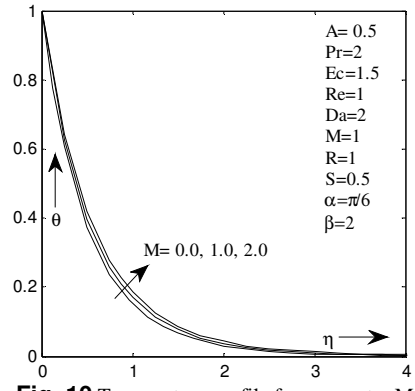

Fig. 10 Temperature profile for parameter M

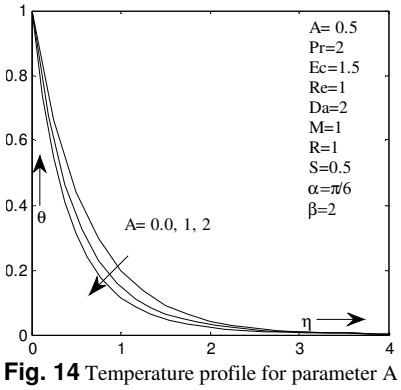

Fig. 14 Temperature profile for parameter A

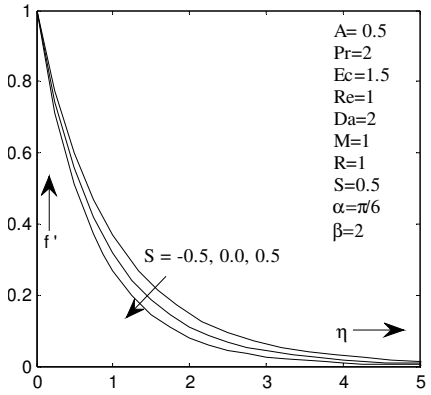

Fig. 15 velocity profile for parameter S

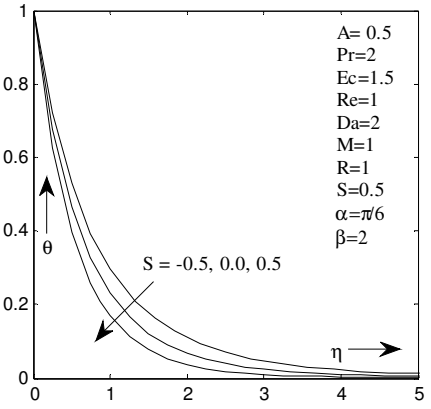

Fig. 16 Temperature profile for parameter S

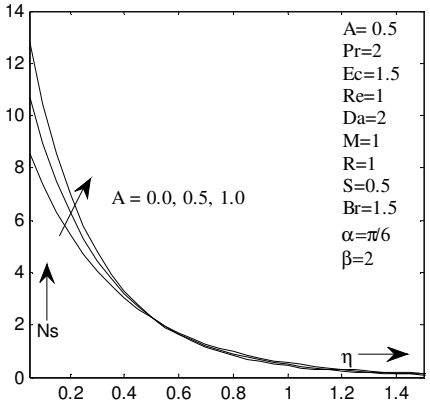

Fig. 17 Entropy profile for parameter A

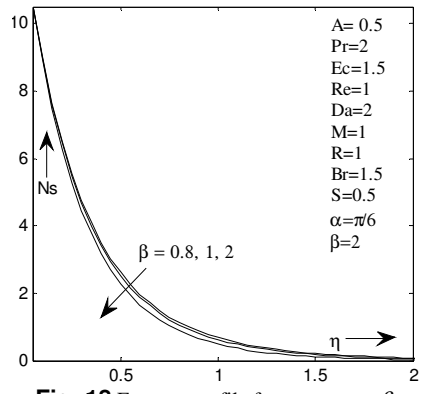

Fig. 18 Entropy profile for parameter β

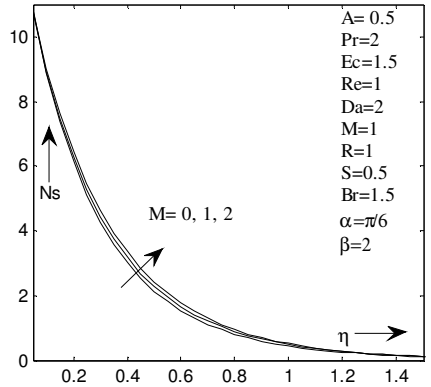

Fig. 19 Entropy profile for parameter M

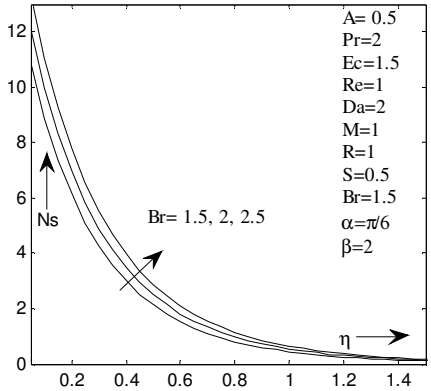

Fig. 20 Entropy profile for parameter Br

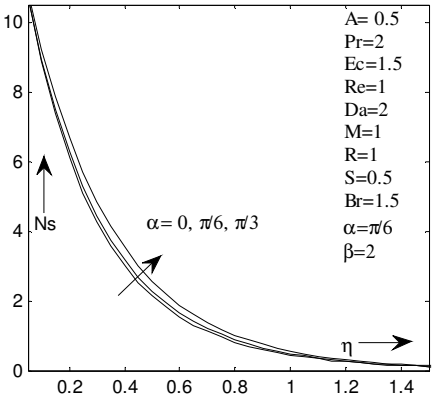

Fig. 21 Entropy profile for parameter α

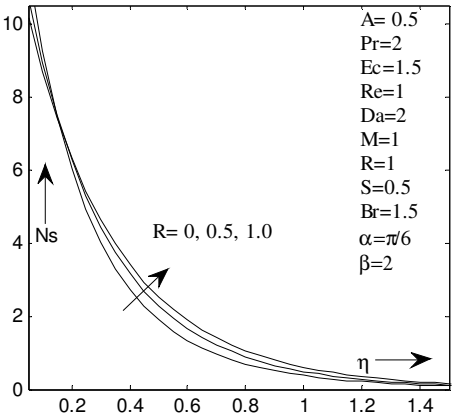

Fig. 22 Entropy profile for parameter R

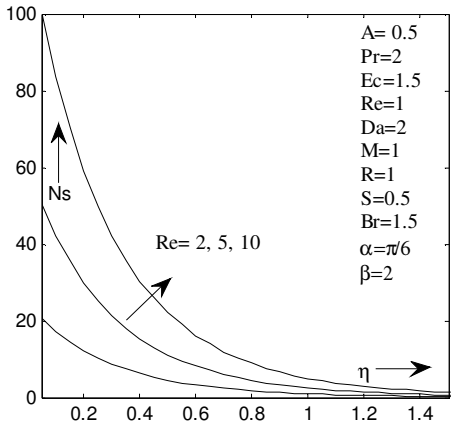

Fig. 23 Entropy profile for parameter Re

7. CONCLUSION

The governing equations of the flow and heat transfer have been solved numerically using R-K forth order with shooting technique. Results obtained with limiting cases are found well in agreement with previously published result. It is observed that

- An increment in unsteady parament, Casson fluid parameter, magnetic field inclined angle decreases the thickness of velocity profile whereas increases in magnetic field parameter it.
- An increment in thermal radiation parameter, Darcy number and Reynolds number increases the thermal boundary layer thickness.
- The skin friction coefficient decreases with increasing unsteadiness parameter.
- An increment in Casson fluid parameter, magnetic field inclined angle, Reynolds number, Brinkmann number increases the thickness of entropy generation profile whereas decreases in unsteady parament it.
- Rising the value of unsteady parameter, inclined angle of magnetic field parameter and magnetic field parameter, reduces the skin friction coefficient.
- Increases inclined angle of magnetic field parameter and magnetic field parameter, reduces the Nusselt number.

ACKNOWLEDGEMENT

We express our sincere gratitude to the reviewer's.

NOMENCLATURE

u, v	velocity components
c_p	specific heat (J/kg·K)
Pr	Prandtl number
k	thermal conductivity (W/m·K)
M	magnetic field parameter
B	magnetic field
R	reflectivity
A	unsteady parameter
t	time (s)
T	temperature (K)
u	interfacial velocity (m/s)
x	coordinate (m)

Greek Symbols

μ	viscosity
ρ	density (kg/m^3)
β	Casson fluid parameter

Subscripts

0	initial condition
∞	ambient environment

References

Bejan A., (1996) "Entropy Generation Minimization". CRC Press. Boca Raton.

Bhatti, M. M., Abbas, T., Rashidi, M., M., Ali, M. E., and Yang, Z., 2016, "Entropy Generation on MHD Eyring–Powell Nanofluid Through a Permeable Stretching Surface," *Entropy*, **18**, 224. https://doi.org/10.3390/e18060224

Chamkha, A.J. Aly, A.M., and Mansour, M.A., 2010, "Similarity Solution for Unsteady Heat and Mass Transfer from a Stretching Surface Embedded in a Porous Medium with Suction/Injection and Chemical Reaction Effects," *Chem. Eng. Commun.*, **197**, 846–858. https://doi.org/10.1080/00986440903359087

Chauhan, D. S., and Kumar, V., 2011a, "Heat Transfer and Entropy Generation During Compressible Fluid Flow in a Channel Partially Filled with a Porous Medium," *International Journal of Energy & Technology*, **3** (14) 1-10.

Chauhan, D. S., and Rastogi, P., 2011b, "Heat Transfer and Entropy Generation in MHD Flow Through a Porous Medium Past a Stretching Sheet," *International Journal of Energy & Technology*, **3** (15) 1-13.

Chauhan, D. S. and Olkha, A., 2011c, "Entropy Generation and Heat Transfer Effects on Non-Newtonian Fluid Flow in Annular Pipe with Naturally Permeable Boundaries," *International Journal of Energy and Technology*, **3** (30) 1-9.

Chauhan, D. S., Rastogi, P., and Agrawal R., 2014, "Magnetohydrodynamic Flow and Heat Transfer in a Porous Medium Along a Stretching Cylinder with Radiation: Homotopy Analysis Method," *Afrika Matematika*, **25**, 115. https://doi.org/10.1007/s13370-012-0102-x

Chauhan, D. S., and Agrawal, R., 2013, "MHD Coupled-Flow and Heat Transfer Across a Porous Layer Due to an Oscillating Plate with Radiation," *Afrika Matematika*, **24** (3) 391-405. https://doi.org/10.1007/s13370-012-0069-7

Chauhan, D. S., and Rastogi, P., 2012, "Unsteady MHD Flow and Heat Transfer Through a Porous Medium Past a Non-Isothermal Stretching Sheet with Slip Conditions," *International Journal of Energy and Technology*, **4** (17) 1-11.

Jain, S., and Bohra, S., 2018a, Hall Current and Radiation Effects on Unsteady MHD Squeezing Nanofluid Flow in a Rotating Channel with Lower Stretching Permeable Wall. Lecture Notes in Mechanical Engineering - Applications of Fluid Dynamics. 127-141.

Jain, S., and Parmar, A., 2018b, Radiation Effect on MHD Williamson Fluid Flow Over Stretching Cylinder Through Porous Medium with

Global Digital Central
ISSN: 2151-8629

Heat Source. Lecture Notes in Mechanical Engineering- Applications of Fluid Dynamics, 61-78.

Jain, S., and Bohra, S., 2017, "Heat and Mass Transfer Over a Three Dimensional Inclined Non-Linear Stretching Sheet with Convective Boundary Conditions" *Indian Journal of Pure and Applied Physics*, **55**, 847-856.

Degan, G., Akowanou, C., And Awanou, N.C., 2007, "Transient Natural Convection Of Non-Newtonian Fluids About A Vertical Surface Embedded In An Anisotropic Porous Medium," *Int. J. Heat Mass Transfer*, **50**, 4629–4639.
https://doi.org/10.1016/j.ijheatmasstransfer.2007.03.023

Kolsi, L., 2016, "MHD Mixed Convection And Entropy Generation In A 3d Lid-Driven Cavity," *Frontiers in Heat and Mass Transfer (FHMT)* 7, 26.
https://doi.org/10.5098/hmt.7.26

Jain, S., Kumar, V., and Bohra, S., 2017, "Entropy Generation for MHD Radiative Compressible Fluid Flow in a Channel Partially Filled with Porous Medium," *Global and Stochastic Analysis*, SI: Pp. 13-31.

Jain, S., and Choudhary, R., 2017, "Soret and Dufour Effects on MHD Fluid Flow Due to Moving Permeable Cylinder with Radiation," *Global and Stochastic Analysis*, SI: pp. 75-84.

Jain, S., 2006, "Temperature Distribution in a Viscous Fluid Flow Through a Channel Bounded by a Porous Medium and a Stretching Sheet". J. Rajasthan Acad. Phy. Sci., 4, 477-482.

Jain, S., and Choudhary, R., 2015, "Effects of MHD on Boundary Layer Flow in Porous Medium Due to Exponentially Shrinking Sheet with Slip," *Procedia Engineering*, **127**, 1203–1210.
https://doi.org/10.1016/j.proeng.2015.11.464

Jangili, S., Gajjela, N, and Anwar Be´G, O., 2016, "Mathematical Modeling of Entropy Generation in Magnetized Micropolar Flow Between Co-Rotating Cylinders with Internal Heat Generation," *Alexandria Engineering J.*, **55**, 1969–1982.
https://doi.org/10.1016/j.aej.2016.07.020

Qing, J., Bhatti, M. M., Abbas, M. A., Rashidi M. M., and Ali, M. E., 2016, "Entropy Generation on MHD Casson Nanofluid Flow Over a Porous Stretching/Shrinking Surface," *Entropy*, **18**, 123.
https://doi.org/10.3390/e18040123

Mabood, F., Shateyi, S., and Khan, W.A., 2015, "Effects of Thermal Radiation on Casson Flow Heat and Mass Transfer Around a Circular Cylinder in Porous Medium," *Eur. Phys. J. Plus,* **130**, 188.
https://doi.org/10.1140/epjp/i2015-15188-y

Layek, G.C., Mukhopadhyay, S. De, P.R., and Bhattacharyya, K., 2013, "Casson Fluid Flow Over An Unsteady Stretching Surface," *Ain Shams Eng. J.*, **4**, 933–938.
https://doi.org/10.1016/j.asej.2013.04.004

Oueslati, F. And Beya, B. B., (2017a) "Magnetoconvection and Irreversibility Phenomena within a Lid Driven Cavity Filled with Liquid Metal Under Magnetic Field," FHMT **8**, 38.
https://doi.org/10.5098/hmt.8.38

Oueslati, F. and Beya, B. B., 2017b, "Analysis of Thermosolutal Natural Convection and Entropy Generation within a Three-Dimensional Inclined Cavity with Various Aspect Ratios," *Journal of Thermal Science and Technology*, **12**(2), JTST0017
https://doi.org/10.1299/jtst.2017jtst0017

Oueslati, F. and Beya, B. B., (2017c) "Numerical Prediction of 3D Thermosolutal Natural Convection and Entropy Generation Phenomena within a Tilted Parallelepipedic Cavity with Various Aspect Ratios," *Computational Thermal Sciences*, **9** (4) 363-382.
https://doi.org/10.1615/ComputThermalScien.2017019810

Oyelakin, I. S., Mondal, S., and Sibanda, P., 2016, "Unsteady Casson Nanofluid Flow Over a Stretching Sheet with Thermal Radiation, Convective and Slip Boundary Conditions," *Alexandria Engineering J.*, **55**, 1025–1035.
https://doi.org/10.1016/j.aej.2016.03.003

Reddy, M. G., 2015, "Unsteady Radiative-Convective Boundary-Layer Flow of a Casson Fluid with Variable Thermal Conductivity," *Journal of Engineering Physics and Thermophysics,* 88, pp. 240-151.
https://doi.org/10.1007/s10891-015-1187-5

Sharidan, S., Mahmood, T., and Pop, I., 2006, "Similarity Solutions for the Unsteady Boundary Layer Flow and Heat Transfer Due to a Stretching Sheet," *Int. J. Appl. Mech. Eng.*, 11, 647–654.